Biosensors

International Edition: DOI: 10.1002/anie.201505179
German Edition: DOI: 10.1002/ange.201505179

A Modular, DNA-Based Beacon for Single-Step Fluorescence Detection of Antibodies and Other Proteins

Simona Ranallo, Marianna Rossetti, Kevin W. Plaxco, Alexis Vallée-Bélisle, and Francesco Ricci**

Abstract: *A versatile platform for the one-step fluorescence detection of both monovalent and multivalent proteins has been developed. This system is based on a conformation-switching stem–loop DNA scaffold that presents a small-molecule, polypeptide, or nucleic-acid recognition element on each of its two stem strands. The steric strain associated with the binding of one (multivalent) or two (monovalent) target molecules to these elements opens the stem, enhancing the emission of an attached fluorophore/quencher pair. The sensors respond rapidly (< 10 min) and selectively, enabling the facile detection of specific proteins even in complex samples, such as blood serum. The versatility of the platform was demonstrated by detecting five bivalent proteins (four antibodies and the chemokine platelet-derived growth factor) and two monovalent proteins (a Fab fragment and the transcription factor TBP) with low nanomolar detection limits and no detectable cross-reactivity.*

Recent years have seen a significant increase in the number of well-characterized biomarkers, proteins present in the blood or on cells that are diagnostic of disease.[1–3] Unfortunately, however, current methods for the detection of such markers are based on either multistep, wash-, or reagent-intensive processes and require sophisticated, laboratory-based measurements (e.g., ELISA or Western blot assays) or are at best only semi-quantitative (e.g., immunochemical dipsticks).[4–6] These drawbacks limit the accessibility of quantitative molecular diagnostics, resulting in delayed treatment, reduced compliance, and poorer outcomes.[1,2,7] In contrast to the cumbersome, multistep nature of current detection schemes, however, biomolecular receptors present in organisms respond to changes in the concentration of their targets in a quantitative fashion and without needing the addition of reagents or wash steps.[8,9] Indeed, these receptors detect thousands of distinct molecules in real time even in the complex in vivo environment.[10] Building artificial biosystems of similar simplicity, convenience, and selectivity represents a major bioengineering goal.

One of the strategies used by naturally occurring "sensors"[11] is based on conformational switching in which a receptor undergoes a large-scale, binding-induced conformational change in the presence of its target.[8,9] As their signaling is linked to a specific, binding-induced event, such "switches" are highly selective and enable detection even in highly complex sample matrices.[10] Moreover, such conformational changes can also be harnessed in artificial systems, where they can be used to generate an optical or electrochemical signal without the addition of exogenous reagents or coupling to exogenous biochemical reactions.[12,13] Motivated by these considerations, we have developed a single-step method for the quantitative detection of specific proteins that is rapid, inexpensive, and highly selective. We drew inspiration from DNA molecular beacons, which are synthetic nucleic acid switches for the detection of specific DNA or RNA sequences that are now widely used for the detection of specific oligonucleotides,[14] and fluorescence resonance energy transfer (FRET) and electrochemical methods for the detection of specific antibodies.[12,15,16]

Molecular beacons are conformation-changing, DNA-based nanoswitches modified with a fluorophore/quencher pair. In the absence of a target, they adopt a stem–loop conformation that opens upon hybridization to their target, thus segregating the reporters and enhancing fluorescence. To create nanoswitches that respond to protein targets instead, we designed a beacon with single-stranded tails appended to each end (Figure 1, left). This allowed us to add recognition elements (hexagons in Figure 1) that specifically bind the protein of interest through conjugation to the appropriate DNA or PNA strand (red strands in Figure 1). Given this structure, the binding of one copy of a bivalent protein (e.g., an antibody) or two copies of one monovalent protein opens the stem, enhancing fluorescence (Figure 1, right).

As a test bed for the optimization of our sensors, we first developed a sensor for antibodies that bind digoxigenin (Dig; Figure 2 A, left). This sensor was obtained by the hybridization of Dig-modified DNA strands to the tailed stem–loop scaffold. The performance of such switches is a function of the stability of their stem.[17] Specifically, an unstable stem partially opens even in the absence of target, thus potentially reducing signal gain. In contrast, an overly stabilized stem reduces affinity (because binding must overcome a higher

[*] S. Ranallo, M. Rossetti, Prof. F. Ricci
Dipartimento di Scienze e Tecnologie Chimiche
University of Rome Tor Vergata
Via della Ricerca Scientifica, Rome 00133 (Italy)
E-mail: francesco.ricci@uniroma2.it
Prof. K. W. Plaxco
Center for Bioengineering & Department of Chemistry and Biochemistry, University of California
Santa Barbara, CA 93106 (USA)
Prof. A. Vallée-Bélisle
Laboratory of Biosensors & Nanomachines
Département de Chimie, Université de Montréal
C.P. 6128, Succursale Centre-ville, Montréal, Québec H3C 3J7 (Canada)
E-mail: a.vallee-belisle@umontreal.ca

Supporting information for this article is available on the WWW under http://dx.doi.org/10.1002/anie.201505179.

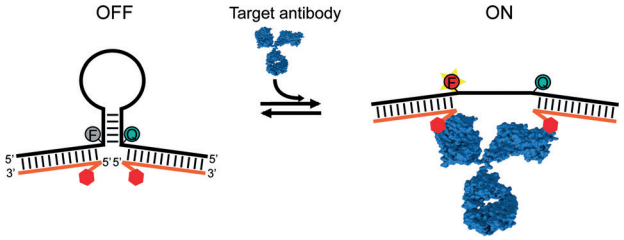

Figure 1. The protein-targeting sensor is composed of a fluorophore/quencher-modified DNA stem–loop system containing two single-stranded tails. To create a target-responsive sensor, these tails are hybridized with DNAs conjugated to an appropriate recognition element (red hexagons). A frame inversion at one tail–stem junction ensures that the two tails meet "head-to-head" (3′-end to 3′-end), thus allowing a single recognition element modified strand sequence to populate both recognition sites. The binding of a bivalent macromolecule (here an antibody) to the two recognition elements opens the stem, allowing for rapid and sensitive protein detection.

barrier). To optimize the sensor performance, we thus synthesized several variants (Figure 2B) differing in the stem stability and loop length (Figure 2C). Melting curves obtained in the absence and presence of saturating target concentrations (Figure 2D; see also the Supporting Information, Figure S1) suggest that a five-base-pair stem with three GC pairs in combination with a 15-base-pair poly-T loop (variant 4) performs particularly well (e.g., 150% gain at saturating target concentrations) at the temperatures of interest for clinical applications (25–35 °C; Figure 2E). Simulations (Nupack)[18] suggest that this construct is stable enough that in the absence of target, 98% of the unbound switches are in their non-emissive stem–loop configuration, maximizing gain without unnecessarily reducing affinity.

The optimized sensor achieves low nanomolar detection limits (Figure 2F). It is noteworthy that the binding curve of the sensor appears to be bilinear rather than hyperbolic (i.e., it is not a Langmuir isotherm). This finding suggests that we are in the "ligand-depletion" (or "tight-binding") regime,[19] where the effective affinity (K_D) for the target is well below the 10 nM switch concentration, and thus each new aliquot of antibody that is added binds to near completion until all of the switches are occupied. Consistent with this, the target concentration at which the observed signal change is half the maximum signal change ($K_{1/2}$) is, at 4.9 ± 2.4 nM, within error of the 5 nM (1/2 of 10 nM) value expected for a stoichiometric 1:1 target-to-sensor ratio. Further confirmation for this was provided by the binding curves collected over a range of sensor concentrations (Figure S2), which always produced $K_{1/2}$ values within error of the value expected for a 1:1 stoichiometry (Figure 2G).

The modular nature of our approach renders it easily applicable to the detection of new proteins through the expedient of changing of its recognition elements (Figure 1). To demonstrate this modularity, we first used recognition elements specific to three monoclonal antibodies: the small molecule dinitrophenol (DNP),[20] the eight-residue FLAG peptide,[21] and a thirteen-residue peptide from the HIV-1 p17 matrix protein.[13d,e] We employed peptide nucleic acid (PNA) rather than DNA strands for the latter two receptors as the

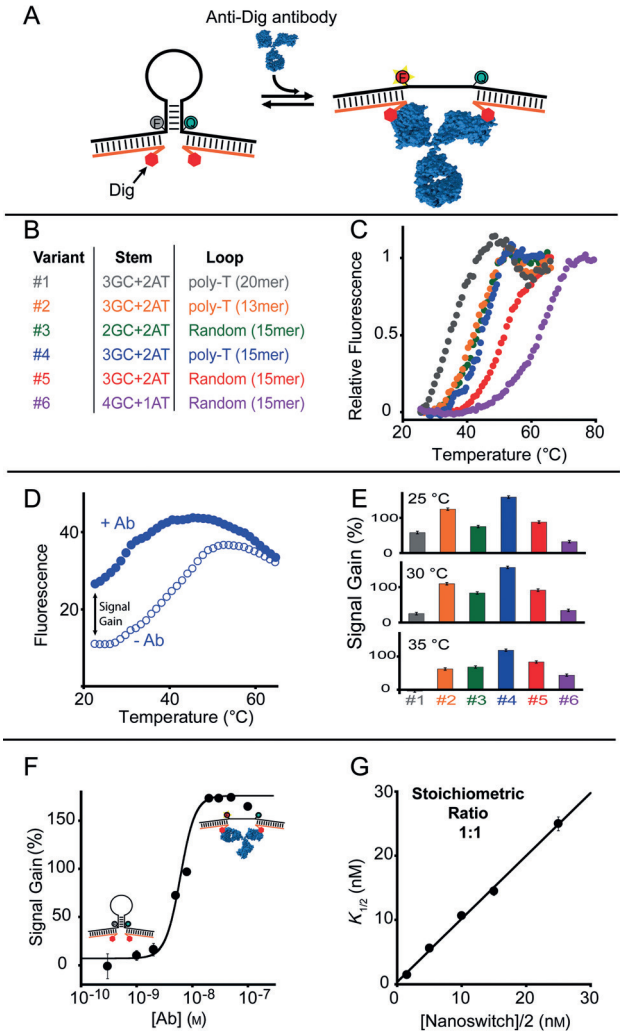

Figure 2. A) Proof-of-principle study with digoxigenin (Dig) as a recognition element for the detection of anti-Dig antibodies. B) Testing of sensors with various stem stabilities induced by variations in the stem GC content (2, 3, or 4) and/or the loop length (13–20 bases). C) Melting curves obtained in the absence of the target illustrate their different stabilities. D) Comparison with curves obtained at a target concentration of 100 nM provides a means of measuring the gain for each variant as a function of temperature. (Under these conditions, antibody binding is effectively temperature-independent; see Figure S7.) E) Sensors of intermediate stability exhibit the best compromise between gain and affinity, with a 3GC stem and a 15-base poly-T loop (variant 4) proving optimal. F) The optimal sensor detects anti-Dig antibodies at low nanomolar concentrations. G) Changes in the $K_{1/2}$ value as a function of the sensors concentration occur in precisely the manner expected for a 1:1 binding stoichiometry, thus supporting the proposed sensing principle. The values shown here and in the following Figures represent averages of three measurements; error bars reflect standard deviations. The binding and melting curves here and in the following Figures were recorded in a solution containing Na_2HPO_4 (50 mM) and NaCl (150 mM) at pH 7.0 with a nanoswitch concentration of 10 nM unless otherwise noted.

synthesis of PNA–peptide chimeras is particularly facile. The stabilities of all three modified stem loops are comparable (Figure S3), and optimal signaling was achieved when using switch variant 4 (Figure S4). Consistent with this, all three sensors responded to their specific targets at low nanomolar

concentrations, with all three $K_{1/2}$ values falling within error of 5 nM (again suggesting that we are in a ligand-depletion regime[19] as the effective affinity of these IgG antibodies is in the low nanomolar regime).[22] All three sensors likewise exhibited similar signal gains (120–150%), suggesting that the construct optimized for the detection of anti-Dig antibodies also performs well for the detection of other antibodies. The sensors appeared to be specific for their target, with none of the three exhibiting any significant cross-reactivity with the other targets (Figure 3A–C). Focusing on the sensor targeting of anti-p17 antibodies (a biomarker for the detection of HIV infections),[1,13e] we found that the detection is also rapid, achieving 90% of the maximum signal after just 2 min (Figure S5, left).

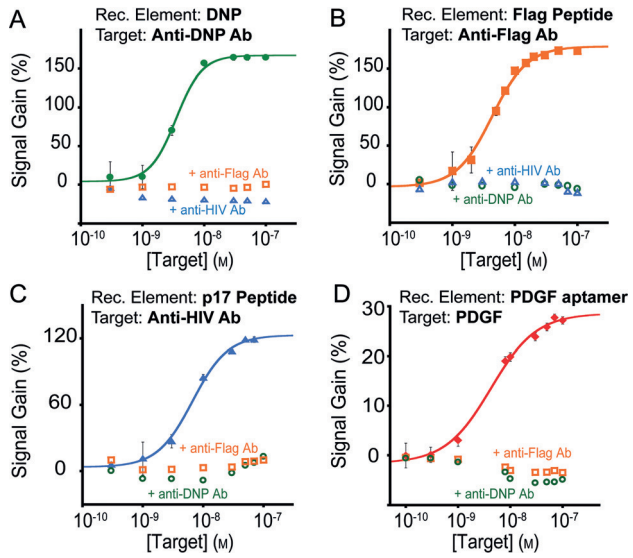

Figure 3. Detection of new targets by changing the recognition element to three different antigens recognized by specific antibodies: A) dinitrophenol (DNP), B) the eight-residue FLAG peptide, and C) a thirteen-residue epitope excised from the HIV protein p17. D) With a 35-base aptamer as the recognition element, the system can also be used to detect the bivalent chemokine PDGF. All four sensors respond to their specific target at low nanomolar concentrations whilst exhibiting no significant response to high concentrations of the targets of other switches.

The binding-induced conformational change that underlies their signaling renders our sensors selective enough to be deployed in complex samples. Our anti-p17 antibody sensor, for example, performed well when used in 90% blood serum, producing a $K_{1/2}$ value within error of that obtained in simple buffer (Figure S5, right). As expected, however, the gain observed under these circumstances is lower owing to the higher background fluorescence of this sample matrix. The other three antibody-detecting sensors also performed well under these traditionally challenging conditions (Figure S6).

Our platform is generalizable to the detection of other (i.e., non-antibody) bivalent proteins. As a proof of concept, we fabricated a sensor displaying two copies of a 35-base aptamer that binds the dimeric-protein platelet-derived growth factor (PDGF) with sub-nanomolar affinity.[23] This sensor recognized its target with a $K_{1/2}$ value of 4.6 ± 2.5 nM, again indicating a one-to-one binding stoichiometry (Figure 3D). It is noteworthy that at a molecular weight of approximately 10 kDa, the aptamer recognition element used in this construct is quite large, corroborating the versatility of our approach. This said, this sensor's 30% gain is rather small compared to those of our antibody-recognizing sensors. We presume this result to be due to one or more of the following: The rather large recognition element might result in 1) a different binding geometry or 2) partial stem opening in the absence of its target (as demonstrated by the melting curves; see Figure S8), and/or 3) the small size of PDGF compared with an antibody may not lead to as great a separation between the quencher and fluorophore upon binding.

Although we initially intended our sensors to detect bivalent proteins, such as antibodies, we also wanted to demonstrate that such systems can nevertheless be used for the detection of monovalent targets if the binding of two molecules of the target produces enough steric hindrance to open the stem. To demonstrate this, we built sensors targeting a Dig-binding Fab fragment and the transcription factor TATA binding protein (TBP), which is recognized by a 20-base, double-stranded hairpin.[13a,b,24] Both sensors respond robustly to their specific targets, albeit with lower gain than our sensors detecting bivalent targets (Figures 4 and S9). The Fab-detecting sensor appears to be operating close to the ligand-depletion regime as the 20 ± 4 nM $K_{1/2}$ value is reasonably close to the 10 nM expected for a 1:2 stoichiometric ratio; binding curves collected over a range of sensor concentrations provide further support for this claim (Figure S10). The 114 ± 5 nM $K_{1/2}$ value of the TBP sensor, in contrast, is far higher than the value that would be expected for a system in the ligand-depletion regime, which is surprising given the 2 nM intrinsic affinity of TBP for its consensus sequence.[24] This result is presumably due to steric effects that reduce the

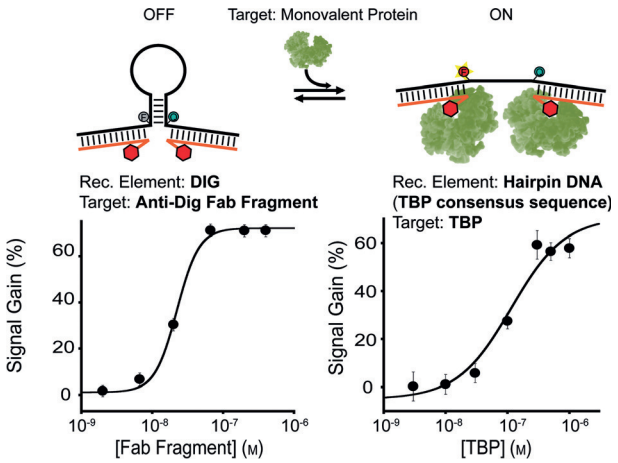

Figure 4. Top: Detection of monovalent targets. The signal change arises from the simultaneous binding of two molecules of the target, which increases steric hindrance, thus opening the stem. Response curves for sensors detecting a monovalent anti-Dig Fab fragment (bottom left) and the monovalent DNA-binding transcription factor TBP (bottom right) are shown. Both sensors readily detect their specific targets at nanomolar concentrations.

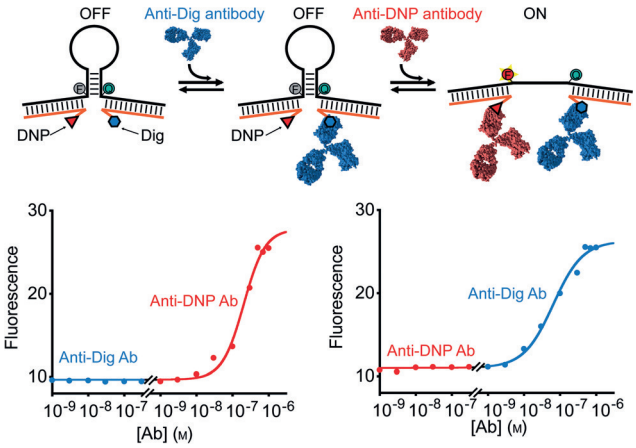

Figure 5. Modular sensors can serve as molecular AND logic gates. Top: Sensor with the recognition elements Dig and DNP. Bottom: Only in the simultaneous presence of both anti-Dig and anti-DNP antibodies, a significant signal increase was observed.

affinity of the protein for its recognition element in these constructs.

Owing to their versatility and modular nature, our sensors can be easily converted into molecular AND logic gates,[25] which signal the concomitant presence of two different macromolecular targets. We therefore fabricated a single sensor presenting both Dig and DNP (Figure 5, top). The addition of either anti-Dig or anti-DNP antibodies on their own does not lead to an increase in fluorescence (Figure 5, bottom). As expected, however, activation is observed when both antibodies are present simultaneously.

In conclusion, drawing inspiration from naturally occurring receptors, which often signal the presence of their molecular target through binding-induced conformational changes, we have developed a new, generalizable, and highly versatile sensing platform for the one-step detection of monovalent and multivalent macromolecular targets. More specifically, we have rationally designed a conformation-switching, optically labelled stem–loop DNA system that supports the introduction of two copies of any of a wide range of polypeptides, small molecules, or oligonucleotide recognition elements. The binding of one (multivalent) or two (monovalent) target molecules to these recognition elements opens the stem, producing a fluorescence signal monotonically related to the concentration of the target. This novel DNA nanoswitch can, in principle, be adapted to the detection of any macromolecular target for which a recognition element can be attached to a DNA or PNA anchoring strand. In support of this claim, we have used our platform to measure the concentrations of five bivalent targets (including four antibodies) and two monovalent protein targets. We detected all seven targets sensitively (at low nanomolar levels) and with excellent specificity (no significant cross-reactivity observed). Finally, the nanoswitches respond rapidly (in less than 10 min) and, owing to the robustness of their structure-switching signaling mechanism, perform well in complex samples matrices, such as blood serum.

Given these attributes, our modular nanoswitches may be advantageous over existing methods for the detection of specific macromolecules. For example, although the lack of any amplification step likely renders our platform less sensitive than ELISA or methods that use binding-induced conformational changes to modulate enzyme activity,[13e,26] the reagent-free, binding-induced signaling mechanism on which our sensors are based drastically simplifies detection by eliminating washing steps and the addition of reagents and by reducing sensitivity to temperature and other environmental factors that influence catalysis. The performance of our system also compares well with other recently developed, similarly homogeneous assays[15,16,26–28] (which are reviewed in Ref. [13d]). Our switch-based approach could nevertheless benefit from further improvements. Its limited dynamic range, for example, could be further extended,[29] and the introduction of FRET-based reporters would support ratiometric measurements that can take into account instrumental and sample-to-sample variations.[30] Nevertheless, we believe that the modularity and convenience of our platform suggests that it may be of utility in a range of applications, including point-of-care diagnostics and in vivo imaging.[10]

Acknowledgements

This work was supported by the European Research Council (ERC, 336493 to F.R.), AIRC (MFAG 14420 to F.R.), the Bill and Melinda Gates Foundation (F.R. and A.V.-B.), the Natural Sciences and Engineering Research Council of Canada (NSERC, 2014-06403 to A.V.-B.), and the National Institutes of Health (AI107936 to K.W.P.).

Keywords: antibodies · aptamers · DNA nanotechnology · fluorescence · molecular devices

How to cite: *Angew. Chem. Int. Ed.* **2015**, *54*, 13214–13218
Angew. Chem. **2015**, *127*, 13412–13416

[1] P. Yager, G. J. Domingo, J. Gerdes, *Annu. Rev. Biomed. Eng.* **2008**, *10*, 107–144.
[2] A. K. Yetisen, M. S. Akram, C. R. Lowe, *Lab Chip* **2013**, *13*, 2210–2251.
[3] E. Fu, P. Yager, P. N. Floriano, N. Christodoulides, J. T. McDevitt, *IEEE Pulse* **2011**, *2*, 40–50.
[4] J. Shen, Y. Li, H. Gu, F. Xia, X. Zuo, *Chem. Rev.* **2014**, *114*, 7631–7677.
[5] A. Ríos, M. Zougagh, M. Avilaa, *Anal. Chim. Acta* **2012**, *740*, 1–11.
[6] R. L. Ornberg, T. F. Harper, H. Liu, *Nat. Methods* **2005**, *2*, 79–81.
[7] a) A. W. Martinez, S. T. Phillips, G. M. Whitesides, E. Carrilho, *Anal. Chem.* **2010**, *82*, 3–10; b) I. S. Park, K. Eom, J. Son, W. J. Chang, K. Park, T. Kwon, D. S. Yoon, R. Bashir, S. W. Lee, *ACS Nano* **2012**, *6*, 8665–8873; c) E. Stern, A. Vacic, N. K. Rajan, J. M. Criscione, J. Park, B. R. Ilic, D. J. Mooney, M. A. Reed, T. M. Fahmy, *Nat. Nanotechnol.* **2010**, *5*, 138–142; d) W. G. Lee, Y. G. Kim, B. G. Chung, U. Demirci, A. Khademhosseini, *Adv. Drug Delivery Rev.* **2010**, *62*, 449–457.
[8] H. Zhang, F. Li, B. Dever, X. F. Li, X. C. Le, *Chem. Rev.* **2013**, *113*, 2812–2841.
[9] A. H. Wu, *Clin. Chim. Acta* **2006**, *369*, 119–124.
[10] a) K. W. Plaxco, H. T. Soh, *Trends Biotechnol.* **2011**, *29*, 1–5; b) A. Vallée-Bélisle, K. W. Plaxco, *Curr. Opin. Struct. Biol.* **2010**,

20, 518 – 526; c) J. H. Ha, S. N. Loh, *Chem. Eur. J.* **2012**, *18*, 7984 – 7999.
[11] a) F. Inci, O. Tokel, S. Wang, U. A. Gurkan, S. Tasoglu, D. R. Kuritzkes, U. Demirci, *ACS Nano* **2013**, *7*, 4733 – 4745; b) M. M. Stratton, S. N. Loh, *Protein Sci.* **2011**, *20*, 19 – 29; c) O. Laczka, R. M. Ferraz, N. Ferrer-Miralles, A. Villaverde, F. X. Munoz, F. J. Del Campo, *Anal. Chim. Acta* **2009**, *641*, 1 – 6; d) D. R. Walt, *ACS Nano* **2009**, *3*, 2876 – 2880.
[12] A. Vallée-Bélisle, F. Ricci, T. Uzawa, F. Xia, K. W. Plaxco, *J. Am. Chem. Soc.* **2012**, *134*, 15197 – 15200.
[13] a) A. Vallée-Bélisle, A. J. Bonham, N. O. Reich, F. Ricci, K. W. Plaxco, *J. Am. Chem. Soc.* **2011**, *133*, 13836 – 13839; b) A. J. Bonham, K. Hsieh, B. S. Ferguson, A. Vallee-Bélisle, F. Ricci, H. T. Soh, K. W. Plaxco, *J. Am. Chem. Soc.* **2012**, *134*, 3346 – 3348; c) M. Merkx, M. W. Golynskiy, L. H. Lindenburg, J. L. Vinkenborg, *Biochem. Soc. Trans.* **2013**, *41*, 1201 – 1205; d) S. Banala, R. Arts, S. J. A. Aper, M. Merkx, *Org. Biomol. Chem.* **2013**, *11*, 7642 – 7649; e) S. Banala, S. J. A. Aper, W. Schalk, M. Merkx, *ACS Chem. Biol.* **2013**, *8*, 2127 – 2132.
[14] a) S. Tyagi, F. R. Kramer, *Nat. Biotechnol.* **1996**, *14*, 303 – 308; b) S. A. E. Marras, S. Tyagi, F. R. Kramer, *Clin. Chim. Acta* **2006**, *363*, 48 – 60.
[15] M. V. Golynskiy, W. F. Rurup, M. Merkx, *ChemBioChem* **2010**, *11*, 2264 – 2267.
[16] K. J. Cash, F. Ricci, K. W. Plaxco, *Chem. Commun.* **2009**, 6222 – 6224.
[17] A. Vallée-Bélisle, F. Ricci, K. W. Plaxco, *Proc. Natl. Acad. Sci. USA* **2009**, *106*, 13802 – 13807.
[18] J. N. Zadeh, C. D. Steenberg, J. S. Bois, B. R. Wolfe, M. B. Pierce, A. R. Khan, R. M. Dirks, N. A. Pierce, *J. Comput. Chem.* **2011**, *32*, 170 – 173.
[19] B. E. F. de Ávila, H. M. Watkins, J. M. Pingarrón, K. W. Plaxco, G. Palleschi, F. Ricci, *Anal. Chem.* **2013**, *85*, 6593 – 6597.
[20] Z. Eshhar, M. Ofarim, T. J. Waks, *Immunology* **1980**, *124*, 775 – 780.
[21] R. J. White, H. M. Kallewaard, W. Hsieh, A. S. Patterson, J. B. Kasehagen, K. J. Cash, T. Uzawa, H. T. Soh, K. W. Plaxco, *Anal. Chem.* **2012**, *84*, 1098 – 1103.
[22] a) H. S. Jung, T. Yang, M. D. Lasagna, J. J. Shi, G. D. Reinhart, P. S. Cremer, *Biophys. J.* **2008**, *94*, 3094 – 3103; b) G. J. Wegner, H. J. Lee, R. M. Corn, *Anal. Chem.* **2002**, *74*, 5161 – 5168.
[23] a) R. Y. Lai, K. W. Plaxco, A. J. Heeger, *Anal. Chem.* **2007**, *79*, 229 – 233; b) M. Cho, Y. Xiao, J. Nie, R. Stewart, A. Csordas, A. T. Csordas, S. S. Oh, J. A. Thomson, H. T. Soh, *Proc. Natl. Acad. Sci. USA* **2010**, *107*, 15373 – 15378.
[24] D. B. Nikolov, H. Chen, E. D. Halay, A. Hoffman, R. G. Roeder, S. K. Burley, *Proc. Natl. Acad. Sci. USA* **1996**, *93*, 4862 – 4867.
[25] B. M. G. Janssen, M. Van Rosmalen, L. Van Beek, M. Merkx, *Angew. Chem. Int. Ed.* **2015**, *54*, 2530 – 2253; *Angew. Chem.* **2015**, *127*, 2560 – 2563.
[26] a) M. L. Geddie, I. Matsumura, *J. Mol. Biol.* **2007**, *369*, 1052 – 1059; b) R. de Las Heras, S. R. Fry, J. Li, E. Arel, E. H. Kachab, S. L. Hazell, C. Y. Huang, *Biochem. Biophys. Res. Commun.* **2008**, *370*, 164 – 168; c) Y. Ohmuro-Matsuyama, C. I. Chung, H. Ueda, *BMC Biotechnol.* **2013**, *13*, 31; d) D. Legendre, P. Soumillion, J. Fastrez, *Nat. Biotechnol.* **1999**, *17*, 67 – 72.
[27] L. Tian, T. Heyduk, *Anal. Chem.* **2009**, *81*, 5218 – 5225.
[28] K. J. Oh, K. J. Cash, A. A. Lubin, K. W. Plaxco, *Chem. Commun.* **2007**, 4869 – 4871.
[29] A. Vallée-Bélisle, F. Ricci, K. W. Plaxco, *J. Am. Chem. Soc.* **2012**, *134*, 2876 – 2879.
[30] E. A. Jares-Erijman, T. M. Jovin, *Nat. Biotechnol.* **2003**, *21*, 1387 – 1395.

Received: June 6, 2015
Revised: July 20, 2015
Published online: September 4, 2015

